Published in final edited form as:
Phys Med Biol. 2014 May 21; 59(10): 2535–2547. doi:10.1088/0031-9155/59/10/2535.

Response-driven Imaging Biomarkers for Predicting Radiation Necrosis of the Brain

Mohammad-Reza Nazem-Zadeh, Ph.D.[1,4,*], **Christopher H. Chapman, M.S.**[1], **Thomas Chenevert, Ph.D.**[2], **Theodore S. Lawrence, M.D., Ph.D.**[1], **Randall K. Ten Haken, Ph.D**[1], **Christina I. Tsien**[1], and **Yue Cao, Ph.D.**[1,2,3]

[1]Department of Radiation Oncology, University of Michigan, Ann Arbor, Michigan, USA

[2]Department of Radiology, University of Michigan, Ann Arbor, Michigan, USA

[3]Department of Biomedical Engineering, University of Michigan, Ann Arbor, Michigan, USA

[4]Departments of Radiology and Research Administration, Henry Ford Hospital, Detroit, Michigan, USA

Abstract

Purpose—Radiation necrosis is an uncommon but severe adverse effect of brain radiation therapy. Current predictive models based on radiation dose have limited accuracy. We aimed to identify early individual response biomarkers based upon diffusion tensor (DT) imaging and incorporated them into a response model for prediction of radiation necrosis.

Methods and Materials—Twenty-nine patients with glioblastoma received six weeks of intensity modulated radiation therapy (RT) and concurrent temozolamide. Patients underwent DT-MRI scans before treatment, at three weeks during RT, and one, three, and six months after RT. Cases with radiation necrosis were classified based on generalized equivalent uniform dose (gEUD) of whole brain and DT index early changes in the corpus callosum and its substructures. Significant covariates were used to develop normal tissue complication probability models using binary logistic regression.

Results—Seven patients developed radiation necrosis. Percentage changes of radial diffusivity (RD) in the splenium at three weeks during RT and at six months after RT differed significantly between the patients with and without necrosis (p=0.05 and p=0.01). Percentage change of RD at three weeks during RT in the 30 Gy dose-volume of the splenium and brain gEUD combined yielded the best-fit logistic regression model.

Conclusions—Our findings indicate that early individual response during the course of RT, assessed by radial diffusivity, has the potential to aid in predicting delayed radiation necrosis, which could provide guidance in dose-escalation trials.

[*]Corresponding Author: Mohammad-Reza Nazem-Zadeh, Ph.D., One Ford Place, Detroit, Michigan, USA, 48202., mohamadn@rad.hfh.edu, Phone: (313) 874-4349.

Conflict of Interest Notification:
The authors report no actual or potential conflicts of interest.

Introduction

Normal brain tissue necrosis after radiation therapy (RT) was an uncommon but severe adverse event in the pre-temozolomide era using the conventional total dose and fractionation schedule to treat glioblastoma. However, with concurrent temozolomide, radiation necrosis is more likely to occur and can occur sooner.[1] Radiation necrosis is largely confined to white matter, often irreversible and progressive, and associated with focal neurological deficits.[1] Radiation necrosis is pathologically associated with hemorrhagic coagulative necrosis.[1] Currently, there is no satisfactory method to predict radiation necrosis.[1–3]

Normal tissue complication probability (NTCP) models of brain radiation necrosis, primarily based upon dose and dose-volume,[3] have been proposed to guide safe delivery of radiation for brain tumor treatment. However, dose-based models have limited predictive capability due to individual patient sensitivity to radiation.[4] Individual brain normal tissue radiation sensitivity could be assessed by an imaging biomarker after starting RT.[5] Diffusion tensor magnetic resonance imaging (DT-MRI), which measures anisotropic diffusion of water molecules in tissue, is sensitive to radiation damage in white matter.[6] Changes in axial and radial diffusivity of white matter are typically considered to reflect axonal damage and demyelination, respectively.[7] Therefore, we hypothesized that early white matter response to radiation measured by DT indices could be an indicator for individual sensitivity to radiation, which could be incorporated into a model for prediction of radiation necrosis.

In this study, we assessed DT index changes only in the corpus callosum, which were taken to be representative of global white matter radiation sensitivity. We chose the corpus callosum because it is the largest white matter structure, centrally located in the brain, and sensitive to radiation. This approach was chosen rather than imaging the normal tissue in the high-dose region because that tissue may be involved with infiltrating tumor cells affecting diffusivity, because radiation necrosis may occur outside of the high-dose region, and because a previous study has shown significant diffusion changes even in normal-appearing white matter distant to the tumor.[2,8] We aimed to develop response models for prediction of radiation necrosis by incorporating white matter response with dose.

Materials and Methods

Patients and Treatment

Patients with histologically-confirmed WHO grade IV gliomas were enrolled in an IRB-approved protocol using concurrent temozolomide and dose-escalated intensity modulated radiation therapy.[9] Gross tumor volume (GTV) was defined as the residual gross tumor or resection cavity from contrast-enhanced T1-weighted MRI. GTVs were expanded uniformly by 1.5 cm to form the clinical target volume (CTV). CTV and GTV were expanded uniformly by 0.5 cm to generate the planning target volumes (PTV1 and PTV2, respectively). RT plans were generated for 30 daily fractions to deliver 60 Gy to PTV1 and a higher total dose to the smaller target PTV2. PTV2 doses of 66 to 81 Gy, assigned to patients by the time-to-event continual reassessment method,[10] were delivered with concurrent daily temozolomide (75 mg/m^2), followed by six cycles of adjuvant

temozolomide (200 mg/m^2 daily x5 days, every 28 days). All patients had baseline MRI scans (pre-RT). Patients who were enrolled in the treatment protocol were eligible to be jointly enrolled in an IRB-approved MRI protocol, in which additional DT-MRI scans were obtained at three weeks during RT, and one, three, and six months after RT.

Radiation Necrosis Diagnosis

Radiation necrosis remains a challenging diagnosis, and the majority of Radiation Therapy Oncology Group (RTOG) trials and others use the working definition of "new symptoms with suggestive radiologic findings", and biopsy is rarely performed.[3] Our study used surgical pathology results to define radiation necrosis, with diagnostic imaging (including PET MRS) and clinical presentation when pathology was not available. Pathologic features consistent with radiation necrosis included vascular hyalinization, coagulative necrosis, and substantial reactive gliosis. Radiation necrosis status was determined before diffusion tensor imaging analysis, and was therefore blinded.

MRI Acquisition

Images were acquired on a 1.5T system (Signa, GE, Milwaukee, USA) for patients enrolled before January 2005, and on a 3T system (Achieva, Philips, Eindhoven, The Netherlands) for patients enrolled afterward. Images included pre- and post-gadolinium T1-weighted, FLAIR T2-weighted, and DT-MRI. Diffusion-weighted images were acquired along 9 gradient directions on the 1.5T scanner, or 15 gradient directions on the 3T scanner with b=1000 s/mm^2, plus a null image with b=0. The acquired image voxel sizes were 1.72×1.72×3.75mm^3 for the 1.5T scanner and 1.75×1.75×2mm^3 for the 3T scanner.

DT Image Pre-Processing

Pre-processing of the diffusion weighted images included rigid body intra- and inter-series co-registration, interpolation to an isometric voxel size of 1.75×1.75×1.75mm^3, and diffusion tensor calculation.[11] Maps of the axial diffusivity (AD; largest eigenvalue of the tensor) and radial diffusivity (RD; mean of two smaller eigenvalues of the tensor) were derived from diffusion tensors.

Segmentation of Corpus Callosum and Substructures

Response to radiation in the corpus callosum that receives doses in all patients was tested as an indicator for individual sensitivity to radiation. The corpus callosum was segmented on each DTI scan for each patient using a level-set algorithm based on tensor similarities between neighboring voxels of a growing surface boundary.[12,13,14] The corpus callosum was further segmented into three substructures of "genu" (rostrum and genu), "body" (rostral body, anterior and posterior mid-body, and isthmus), and "splenium" using Witelson subdivisions.[12,15] After segmentation, co-registered DT, T1-weighted and T2-weighted images were visually inspected for severe edema or image distortion in the corpus callosum substructures. If any substructure was affected by severe edema and/or mass effect, it was excluded from analysis. No patient experienced radiation necrosis in the corpus callosum.

Dosimetric Parameters

To assess the dose effect on development of radiation necrosis, the accumulated radiation dose over 30 fractions in each brain were converted to 2 Gy per fraction equivalent doses with α/β=2.5 Gy. The generalized equivalent uniform dose (gEUD)[16] of the whole brain excluding the gross target volume (GTV) was calculated as

$$gEUD = \sqrt[a]{\sum_{i=1}^{n} p(d_i) d_i^a} \quad (1)$$

where $\boldsymbol{p(d_n)}$ denotes a volume fraction of the brain sub-region receiving dose $\boldsymbol{d_n}$ to the whole brain volume. Our model used a=14, determined from a maximum likelihood analysis of the Lyman NTCP model[17] for radiation necrosis from an earlier dataset of 38 patients (unpublished). After aligning the dose distribution map of each patient to the DT images through rigid co-registration of treatment planning CT with pre-RT T1-weighted images, accumulated dose-volume histograms of the corpus callosum and its substructures were created. DT index changes in the dose-volumes >0, >10, >20, …, >60 Gy were calculated from pre-RT to three weeks during RT, and one, three and six months after RT.

Changes in DT Indices

Longitudinal changes in AD and RD were compared by Student's *t*-test between patients with radiation necrosis and those without radiation necrosis. Correlations between earlier and later DT index changes were examined using linear regression. Significance level was $p<0.05$.

NTCP Prediction Models

To identify candidate variables for prediction of radiation necrosis, we first performed univariate logistic regressions. The tested variables included whole brain gEUD, and the DT response measures of percentage changes in RD or AD in the corpus callosum, any of the substructures, and any of the dose-volumes after starting RT. We then performed multivariate logistic regression using a combination of whole brain gEUD and the DT response measures from the corpus callosum regions with significant univariate models. The logistic model "goodness of fit" of was assessed by deviance (a generalized residual sum of squares). To determine the significance of multivariate regression models, correction for multiple comparisons was performed by a Bonferroni-type sequential procedure to reduce type-I error. A comparison was considered statistically significant when $p_i < \alpha_i$ where p_i is the i^{th} smallest p-value from m comparisons and $\alpha_i = 0.05i/m$.[18] The significant univariate models were then statistically compared with multivariate models.

For better clinical interpretation of the models, a "cutoff value" for predicting radiation necrosis was assigned using receiver operating characteristic (ROC) curves. The cutoff value was assigned to the point where the sum of model sensitivity and specificity was maximal. From this cutoff value, the significance of the classification was tested using the 2×2 classification contingency table (true positives, false positives, true negatives, false negatives) and Fisher's exact test.

Results

Patients and Normal Tissue Complications

Of 34 patients enrolled in the imaging protocol, 29 without severe edema or image distortion in the corpus callosum were analyzed (Table 1). Of 29 patients, 7 had developed normal tissue radiation necrosis between four to eight months after RT, in whom prescribed doses were 78 Gy or higher. Radiation necrosis occurred in the left parietal lobe in 3 patients, right frontal lobe in 2 patients, right temporal lobe in 1 patient, and left occipital lobe in 1 patient, all outside of the corpus callosum (Figure 1). Pathologic radiation necrosis was confirmed by surgical resection in 6 patients while 1 patient's diagnosis was based on imaging and clinical presentation. Two patients had substantive imaging changes leading to surgical resection, but no radiation necrosis was seen on pathology and patients were not clinically symptomatic; they were classified as "no necrosis". The mean whole brain gEUD for patients with necrosis (median 72.5 Gy, range 64.8–75.8 Gy) was significantly greater than for those without (median 68.1 Gy, range 55.4–74.1 Gy) (Table 1, p=0.04), as was the prescription dose (Table 1, p=0.05). There were no associations between radiation necrosis outcome and tumor location, bevacizumab use, or scanner type (Table 1).

Longitudinal Changes in DT Indices of Corpus Callosum

Of 29 patients, all had DT-MRI pre-RT, 17 at three weeks during RT, and 26, 18 and 11 at one, three and six months after RT, respectively. In the splenium, a progressive increase in RD from pre-RT to six months after RT was observed in the patients with necrosis, but not in those without. The mean RD in the splenium of the patients with necrosis increased to +4.3% ±1.6% (SE, standard error) at three weeks during RT, and to +82.2% ±37.7% six months after RT, which were significantly different from the patients without necrosis at three weeks during RT (−5.9% ±5.5%, p=0.049) and six months after RT (−9.6% ±4.7%, p=0.025) (Figure 2A). Similarly, the patients with necrosis showed a progressive increase in AD of the splenium from pre-RT to six months after RT, but those without necrosis had only a minor increase from pre-RT to three months after RT. The AD changes in the splenium were different between the two groups six months after RT (+14.3% ±9.2% vs. −3.4% ±1.9%, p=0.067) (Figure 2B). Regardless of necrosis outcome, the RD and AD changes in the splenium one month after RT were significantly correlated with those three months after RT (AD: R^2=0.79, RD: R^2=0.68; n=15, p<0.001), indicating progressive changes in DTI indices after RT. Average gEUD or fractional dose-volumes in the splenium of necrosis patients was not significantly greater than in non-necrosis patients (Table 1), suggesting that the significantly greater DTI index changes in the splenium of the patients with necrosis are most likely due to greater early sensitivity to radiation which was only identified using DTI. In the genu and body of corpus callosum there were no significant group differences in AD or RD at any time point.

Univariate NTCP Prediction Models

Using dose alone, a gEUD threshold of 69.3 Gy was found marginally significant (n=29, p=0.07, specificity=73%, sensitivity=71%), suggesting a model based on dosimetry parameter alone has limited capability to predict radiation necrosis. Using DT index responses in the splenium at three weeks during RT, necrosis cases were significantly

predicted by positive RD changes in the whole splenium (n=17, p=0.043) and in the 10 Gy dose-volume (n=16, p=0.034), and marginally in the 30 and 40 Gy dose-volumes (Table 2), which were candidate variables for multivariate predictive models. However, necrosis was not significantly predicted by any DT index changes in the splenium or its subvolumes one or three months after RT. Although the predictive value was diminished six months after RT since some patients had already developed radiation necrosis but the radiographic diagnostic value without surgery exists, necrosis was significantly determined by RD changes at six months in the whole splenium (n=11, p=0.015), 10 Gy dose-volume (n=11, p=0.015), and 20 Gy dose-volume of the splenium (n=10, p=0.048). For comparison, brain gEUD predictions were attempted using only patients with DT index changes available at three weeks during RT and six months after RT in different dose-volumes of the splenium. None of gEUD predictions in any of dose-volume of the splenium reached significance (Table 2).

Multivariate Radiation Necrosis Prediction Models

Combining brain gEUD with DT indices, radiation necrosis cases were significantly predicted by brain gEUD and the RD percentage change in the splenium dose-volumes of 10, 20, 30, 40, 50, or 60 Gy at three weeks during RT and six months after RT, after correcting for multiple comparisons (Table 2). The best classification occurred at three weeks during RT from adding RD percentage change in the 15 patients with 30 Gy dose-volume available, with specificity= 83% and sensitivity=78% (p=0.007, Figure 3B, Table 2A). Although radiation necrosis cases were not significantly classified by any AD changes alone, combining brain gEUD and AD percentage changes in the splenium dose-volumes of 30, 40, 50 Gy, or 60 Gy at three weeks during RT resulted in classifications with $p \leq 0.04$, but not significant after correcting for multiple comparisons (Table 2). The best AD classification resulted from using the AD change in the 50 Gy dose-volume available, with specificity= 75% and sensitivity=67% (p=0.010, Table 2A). We define the Response Models 1, 2, and 3 as the percentage RD change in splenium 30 Gy dose-volume at three weeks during RT, the percentage AD change in splenium 50 Gy dose-volume at three weeks during RT, and the percentage RD change in splenium 30 Gy dose-volume at six months after RT, respectively. Response Model 3 resulted in 100% sensitivity and 100% specificity for the 8 patients with 30 Gy dose-volume available (p=0.036, Figure 3D, Table 2B), which could be valuable for radiographic necrosis diagnosis without surgery. However, the percentage AD change in splenium 50 Gy dose-volume did not give significant classification at six months after RT (Table 2B).

Comparing multivariate and univariate NTCP response Models

Using brain gEUD from all 29 patients, the NTCP model had a deviance of 27.6 (n=29, Figure 3A). In Response Model 1 using both brain gEUD and RD percentage change in the 30 Gy dose-volume of the splenium at three weeks during RT, the NTCP model yielded a deviance of 15.6 (n=15, Table 3, Figure 3B), compared to a deviance of 17.8 from a model using brain gEUD alone from the same 15 patients (Figure 3C). The added predictive value of the early RD changes in the splenium was non-significant (p=0.13). In Response Model 2, using both brain gEUD and AD percentage changes at three weeks during RT in the 50 Gy dose-volume of the splenium, the NTCP model fitting yielded a deviance of 15.9 (n=14, Table 3), compared to a deviance of 16.9 from a model using brain gEUD alone from the

same 14 patients, also a non-significant improvement (p=0.32). All the fitted coefficients of the predictors and their significance are given in Table 3.

Discussion

In this study, we investigated whether early DT index response in the corpus callosum of the patients who had glioblastoma and were treated by concurrent temozolomide and dose-escalated RT could predict risk for delayed normal brain radiation necrosis. We found a significant increase of radial diffusivity in the splenium of patients with radiation necrosis as early as at three weeks during RT compared to those without. Incorporating the early response of DT indices in the splenium at three weeks during RT with brain gEUD resulted in better prediction of radiation necrosis, yet the improvement was not statistically significant. However, this study generates a hypothesis that DT-MRI could add discriminatory information in the NTCP model for radiation necrosis prediction and diagnosis, which has the potential to provide guidance for complication risk management of patients in dose-escalation trials.[5] Furthermore, our study suggests there are predictive changes in white matter integrity beyond the future location of radiation necrosis, and that the corpus callosum can be used as a surrogate location for predictive DT index changes. This is advantageous because DT index analysis of a single location can be more easily standardized and quickly collected with automated contouring techniques.

We first characterized the DT index changes in the corpus callosum and its substructures over time for patients with and without radiation necrosis to identify candidate surrogates for prediction of radiation necrosis. Although the actual location of necrosis within the brain may show early imaging changes, this location is not known before necrosis occurs. Our approach was to identify a structure that receives sufficient dose and is sensitive to radiation as a surrogate for prediction of necrosis. We found progressive increases in RD of the splenium in patients with necrosis but not in those without up to six months after RT, even though the splenium in the first group received only marginally greater doses than the latter group. Although necrosis did not occur in the splenium, the 80% increase in RD of the necrosis group six months after RT suggests that the splenium is a sensitive structure to radiation. AD increased much less than RD, indicating demyelination is the predominant early radiation effect. The early differences in the DT index changes between the patients with and without necrosis suggest a basis for early classification. Due to the variation of the doses received in the whole splenium, we tested DT index changes in several dose-volumes (10 Gy to 60 Gy) for prediction of radiation necrosis. The central location of the splenium warrants a large portion of it receiving dose regardless of tumor location; in our sample 15/17 patients received sufficient dose (30 Gy) in the splenium to allow this comparison.

The increased risk of radiation necrosis with high-dose RT has been demonstrated previously.[3,4] Similarly, in our study necrosis only occurred in subjects who received prescription doses ≥78 Gy. However, using gEUD to account for the dose-volume effect in the brain, we found that there was substantial overlap of brain gEUD between cases with and without necrosis (Table 1), suggesting differences in individual sensitivity to radiation. Combining early changes in DT indices of the splenium as a radiation response measure with whole brain gEUD resulted in a better separation of cases with necrosis from those

without, however the improvement of the logistic models was not statistically significant. Further validation may show that a model built on response measures has the potential to aid in physiological adaptive RT.

One limitation of this study is missing follow-up images. However, at three weeks during RT, when the earliest and best predictive capability was seen, imaging data was available for six of seven necrosis patients. Another limitation is that patients were imaged on two different scanners, which could contribute some variation in diffusion indices.[19,20] To reduce measurement error, each patient completed follow-up imaging on a single scanner. No systematic difference in DT index changes was seen between scanner types, suggesting that our method is appropriate for the different magnet strengths in common clinical use (1.5T and 3T). Finally, the sample size of our study is small. However, important observations made in this study could serve as the basis for larger confirmatory studies. We found that a range of dose-volumes clustered between 30–50 Gy was useful for response measurement, indicating a robust association rather than random occurrence.

A normal tissue complication imaging biomarker could have direct clinical impact. In a recent trial, efforts to improve glioblastoma survival using dose-escalation and concurrent chemotherapy were hampered by radiation necrosis in patients with prescription doses >75 Gy.[9] However, in that trial 83% of patients receiving >75 Gy did not experience necrosis. There was also a significant reduction in central treatment failure at higher doses. If it were possible to escalate dose only in patients with a low risk of radiation necrosis, the overall therapeutic index of treatment could be improved. For dose-planning, one could use the logistic response model incorporating gEUD and splenium ΔRD% at 3 weeks (Table 3) and restrict prescription dose and gEUD only to a predetermined necrosis probability threshold. Future prospective studies may validate this concept.

Dose parameters alone have limited ability to predict radiation necrosis risk at the individual level.[3] Our alternative strategy is to use the individual radiation response measured by diffusion tensor imaging as a predictor. This variable can contribute information about individual radiation response in the setting of complex interactions with dose and clinical risk factors, possibly bypassing the need to account for each of these. Our study has shown promising evidence that longitudinal diffusion tensor imaging changes could improve a predictive model for radiation necrosis even before the delivery of the total radiation dose, when adjustment of the treatment plan would still be possible and the patient can benefit from decreased radiation necrosis risk.

Acknowledgments

Financial Support:

NIH grants RO1 NS064973, 3PO1 CA59827, and 2PO1 CA85878.

References

1. Fink J, Born D, Chamberlain MC. Radiation necrosis: relevance with respect to treatment of primary and secondary brain tumors. Curr Neurol Neurosci Rep. 2012; 12:276–285. [PubMed: 22350279]

2. Sundgren PC, Cao Y. Brain irradiation: effects on normal brain parenchyma and radiation injury. Neuroimaging clinics of North America. 2009; 19:657–668. [PubMed: 19959011]
3. Lawrence YR, et al. Radiation dose-volume effects in the brain (QUANTEC). Int J Radiat Oncol Biol Phys. 2010; 76:S20–7. [PubMed: 20171513]
4. Kehwar TS. Analytical approach to estimate normal tissue complication probability using best fit of normal tissue tolerance doses into the NTCP equation of the linear quadratic model. J Cancer Res Ther. 2005; 1:168–179. [PubMed: 17998649]
5. Jeraj R, Cao Y, Haken, Ten RK, Hahn C, Marks L. Imaging for assessment of radiation-induced normal tissue effects. Int J Radiat Oncol Biol Phys. 2010; 76:S140–4. [PubMed: 20171509]
6. Assaf Y, Pasternak O. Diffusion tensor imaging (DTI)-based white matter mapping in brain research: a review. J Mol Neurosci. 2008; 34:51–61. [PubMed: 18157658]
7. Song SK, et al. Diffusion tensor imaging detects and differentiates axon and myelin degeneration in mouse optic nerve after retinal ischemia. Neuroimage. 2003; 20:1714–1722. [PubMed: 14642481]
8. Sundgren PC, et al. Differentiaion of recurrent brain tumor versus radiation injury using diffusion tensor imaging in patients with new contrast-enhancing lesions. Magnetic Resonance Imaging. 2006; 24:1131–1142. [PubMed: 17071335]
9. Tsien CI, et al. Concurrent temozolomide and dose-escalated intensity-modulated radiation therapy in newly diagnosed glioblastoma. Clin Cancer Res. 2012; 18:273–279. [PubMed: 22065084]
10. Normolle D, Lawrence T. Designing dose-escalation trials with late-onset toxicities using the time-to-event continual reassessment method. J Clin Oncol. 2006; 24:4426–4433. [PubMed: 16983110]
11. Nazem-Zadeh MR, Chapman CH, Lawrence TL, Tsien CI, Cao Y. Radiation therapy effects on white matter fiber tracts of the limbic circuit. Med Phys. 2012; 39:5603. [PubMed: 22957626]
12. Nazem-Zadeh MR, et al. Segmentation of corpus callosum using diffusion tensor imaging: validation in patients with glioblastoma. BMC Med Imaging. 2012; 12:10. [PubMed: 22591335]
13. Nazem-Zadeh MR, Davoodi-Bojd E, Soltanian-Zadeh H. Level set fiber bundle segmentation using spherical harmonic coefficients. Computerized Medical Imaging and Graphics. 2010; 34:192–202. [PubMed: 19846274]
14. Nazem-Zadeh MR, Davoodi-Bojd E, Soltanian-Zadeh H. Atlas-based fiber bundle segmentation using principal diffusion directions and spherical harmonic coefficients. NeuroImage. 2011; 54:S146–S164. [PubMed: 20869453]
15. Witelson SF. Hand and sex differences in the isthmus and genu of the human corpus callosum. A postmortem morphological study. Brain. 1989; 112 (Pt 3):799–835. [PubMed: 2731030]
16. Niemierko A. A generalized concept of equivalent uniform dose (EUD). Med Phys. 1999; 26:1101.
17. Lyman JT. Complication probability as assessed from dose-volume histograms. Radiat Res Suppl. 1985; 8:S13–9. [PubMed: 3867079]
18. Benjamini Y, Hochberg Y. Controlling the false discovery rate: a practical and powerful approach to multiple testing. Journal of the Royal Statistical Society. Series B (Methodological). 1995:289–300.
19. Vollmar C, et al. Identical, but not the same: intra-site and inter-site reproducibility of fractional anisotropy measures on two 3.0T scanners. Neuroimage. 2010; 51:1384–1394. [PubMed: 20338248]
20. Nazem-Zadeh MR, Chapman CH, Lawrence TS, Tsien CI, Cao Y. Uncertainty in assessment of radiation-induced diffusion index changes in individual patients. Phys Med Biol. 2013; 58:4277–4296. [PubMed: 23732399]

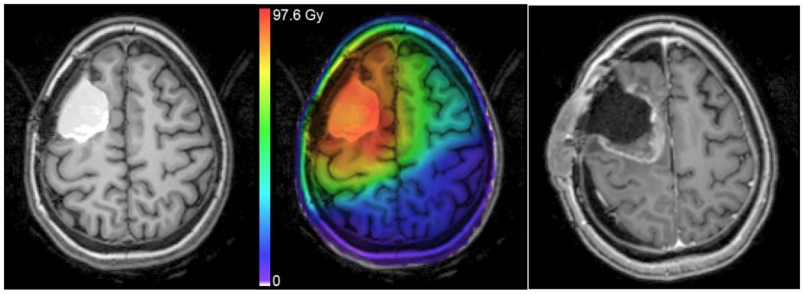

Figure 1.

Left: T1-weighted post-contrast MRI showing hemorrhage in resection cavity before RT. Middle: Registered treatment planning dose map overlay. Color scale units biologically corrected to 2 Gy fractions using $\alpha/\beta = 2.5$ for late effects. Right: T1-weighted post-contrast MRI at 9 months after RT showing radiation necrosis, later confirmed by surgical pathology.

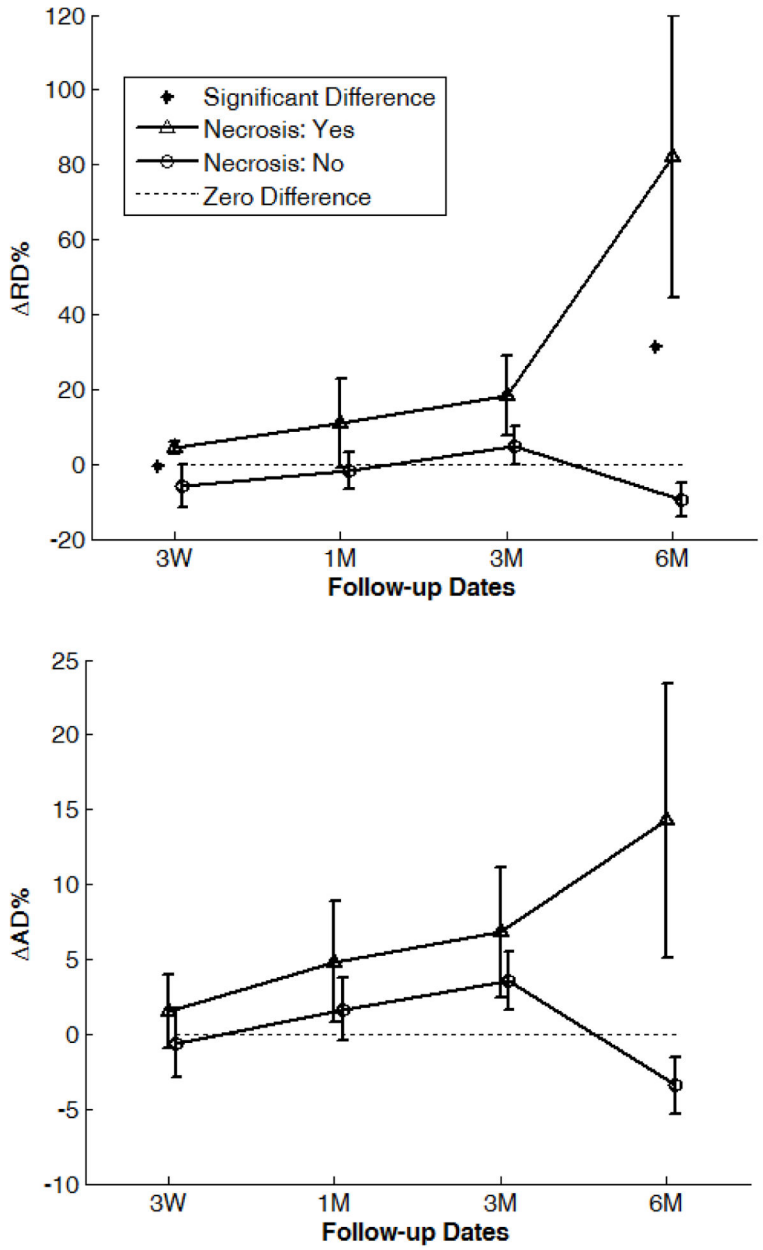

Figure 2.

Percentage changes in (a) RD and (b) AD in the corpus callosum splenium by time point and normal tissue complication status. Error bars are standard error.

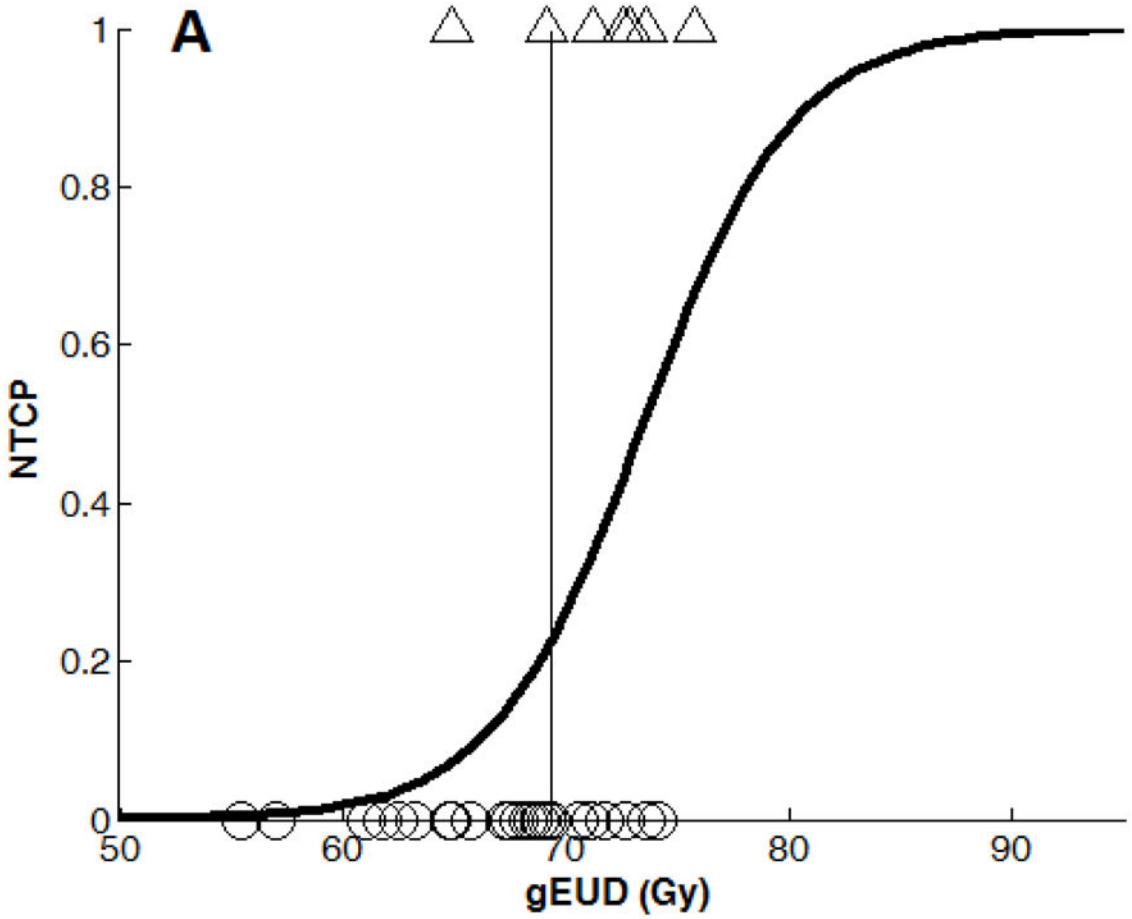

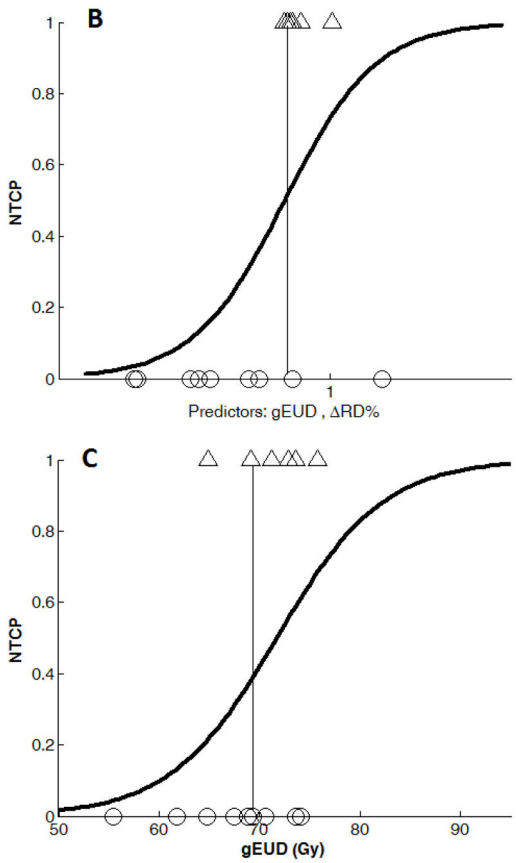

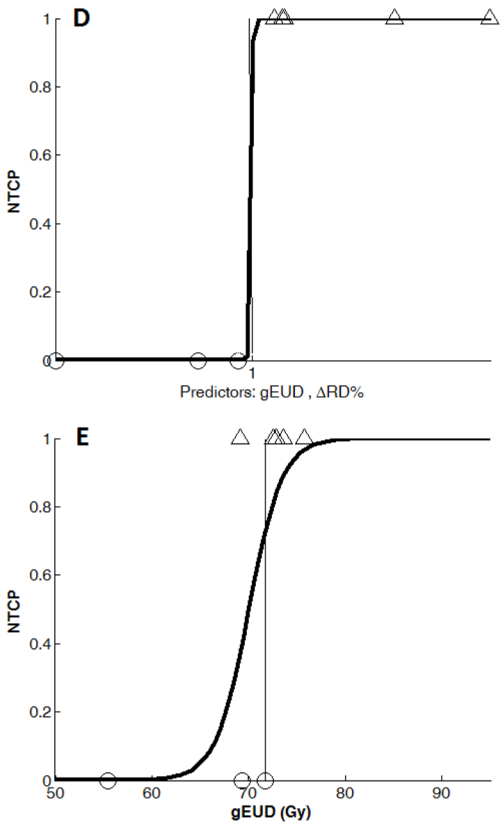

Figure 3.

Binary logistic regression NTCP models using (**A**): gEUD alone (n=29), (**B**): **Combined** gEUD and the RD changes in the splenium dose-volume of 30 Gy at three weeks during RT (**Response Model 1,** n=15), (**C**): gEUD alone from the patients in (**B**), n=15), (**D**): **Combined** gEUD and the RD changes in the splenium dose-volume of 30 Gy at 6 months after RT (n=8), and (**E**): gEUD alone from the patients in (d) (n=8).

Note that the x-axis variable in (B) and (D) is $x = a + b \times gEUD + c \times \Delta RD\%$ with different estimations of a, b, and c coefficients at three weeks and 6 months after RT (See Table 3).

Table 1

Patient characteristics by normal tissue complication status.

	Necrosis: No	Necrosis: Yes	*p*-value
n	22	7	
Female	11 (50%)	4 (57%)	0.75
Median age; range (years)	62; 22–78	44; 31–75	0.27
Median prescription dose to PTV2; fraction (Gy)	75; 2.5	78; 2.6	0.05
Median whole brain gEUD (range) (Gy)	68.1 (55.4–74.1)	72.5 (64.8–75.8)	0.04
Received bevacizumab	6 (27.2%)	1 (14.3%)	0.65
Frontal tumor	2 (9.1%)	2 (28.6%)	0.30
Occipital tumor	2 (9.1%)	2 (28.6%)	0.30
Parietal tumor	5 (22.7%)	1 (14.3%)	0.61
Temporal tumor	13 (59.1%)	2 (28.6%)	0.16
3T MRI scanner	14 (63.3%)	3 (42.9%)	0.36
Mean splenium gEUD Gy (SE)	49.3 (4.8)	63.8 (5.7)	0.13
10-Gy splenium dose-volume % (SE)	84.1 (5.5)	99.0 (0.4)	0.10
20-Gy splenium dose-volume % (SE)	66.1 (7.9)	84.7 (3.5)	0.14
30-Gy splenium dose-volume % (SE)	57.6 (8.2)	69.4 (5.6)	0.26
40-Gy splenium dose-volume % (SE)	47.3 (7.7)	58.7 (6.6)	0.26
50-Gy splenium dose-volume % (SE)	38.8 (7.3)	47.8 (7.5)	0.30
60-Gy splenium dose-volume % (SE)	26.3 (6.6)	38.1 (8.3)	0.24

SE: standard error.

Table 2

Fisher's exact test p-values from classifications

(A) Three weeks during RT					
Splenium Subvolume	**RD**	**gEUD**	**RD + gEUD**	**AD + gEUD**	**Sample *n***
Whole	0.043*	**1.0**	0.131	0.131	17
>10 Gy	0.034*	**0.299**	0.034*^	0.145	16
>20 Gy	0.145	**0.299**	0.034*^	0.608	16
>30 Gy	0.119	**0.329**	0.007*^	0.028*	15
>40 Gy	0.119	**0.329**	0.007*^	0.041*	15
>50 Gy	0.138	**0.277**	0.010*^	0.010*	14
>60 Gy	0.242	**1.0**	0.028*^	0.028*	12

(B) Six months after RT					
Splenium Subvolume	**RD**	**gEUD**	**RD + gEUD**	**AD + gEUD**	**Sample *n***
Whole	0.015*	**0.242**	0.151	0.061	11
>10 Gy	0.015*	**0.242**	0.151	0.061	11
>20 Gy	0.048*	**0.206**	0.008*^	0.167	10
>30 Gy	0.196	**0.571**	0.036*^	1.0	8
>40 Gy	0.196	**0.571**	0.036*^	0.571	8
>50 Gy	0.196	**0.571**	0.036*^	0.1	8
>60 Gy	0.40	**1.0**	0.2	0.4	5

gEUD from whole brain and DT index changes in the splenium from pre-RT to (A) three weeks during RT and (B) six months after RT. For comparison, gEUD classifications include the same patients as the matching DT index model.

* $p<0.05$ by Fisher's exact test.

^ Significant using the Bonferroni-type sequential procedure for multiple comparisons.

Table 3

NTCP Logistic Regression Models

Model	Predictor Coefficients	Deviance	Sample *n*
gEUD model (all patients): $x = a + b \times gEUD$	***a*=−2.19 (p=0.04),** *b* = 0.298 ***Gy*$^{-1}$**(p=0.049), *cut-off value=69.3*	27	29
Response Model 1: $x = a + b \times gEUD + c \times \Delta RD\%$ gEUD comparison 1:	***a*=−1.38 (p=0.20),** *b* = 0.193 ***Gy*$^{-1}$**(p=0.21), *c* = 0.059 (p=0.20), *cut-off value=0.05*	15.6	15
	***a*=−1.36 (p=0.18),** *b* = 0.189 ***Gy*$^{-1}$**(p=0.19), *cut-off value=69.3*	17.8	15
Response Model 2: $x = a + b \times gEUD + c \times \Delta AD\%$ gEUD comparison 2:	***a*=−1.48 (p=0.17),** *b* = 0.209 ***Gy*$^{-1}$**(p=0.17), *c* = 0.075(p=0.35), *cut-off value=0.27*	15.9	14
	***a*=−1.27 (p=0.20),** *b* = 0.179 ***Gy*$^{-1}$**(p=0.20), *cut-off value=70.6*	16.9	14
Response Model 3: $x = a + b \times gEUD + c \times \Delta RD\%$ gEUD comparison 3:	***a*=−1022.1 (p=0.94), *b* = 14.14 *Gy*$^{-1}$ (p=0.94), *c* = 1.06 (p=0.94), *cut-off value=1.15***	**1.9e-6**	**8**
	a*=−40.84 (p=0.26), *b* = 0.583 *Gy*$^{-1}$ (p=0.25) *cut-off value=71.7	**6.7**	**8**

Response Model 1: percentage RD change in splenium 30 Gy dose-volume at three weeks during RT

Response Model 2: percentage AD change in splenium 50 Gy dose-volume at three weeks during RT

Response Model 3: percentage RD change in splenium 30 Gy dose-volume at six months after RT

gEUD comparisons performed using same patients available for response models. Deviance is generalized residual sum of squares, a measure of model goodness-of-fit. *x* is the logit function of the fitted NTCP probability.